

Searching for Chameleon-like Scalar Fields

Sergei A. Levshakov, Paolo Molaro, Mikhail G. Kozlov, Alexander V. Lapinov,
Christian Henkel, Dieter Reimers, Takeshi Sakai and Irina I. Agafonova

Abstract Using the 32-m Medicina, 45-m Nobeyama, and 100-m Effelsberg telescopes we found a statistically significant velocity offset $\Delta V \approx 27 \pm 3 \text{ m s}^{-1}$ (1σ) between the inversion transition in $\text{NH}_3(1,1)$ and low- J rotational transitions in $\text{N}_2\text{H}^+(1-0)$ and $\text{HC}_3\text{N}(2-1)$ arising in cold and dense molecular cores in the Milky Way. Systematic shifts of the line centers caused by turbulent motions and velocity gradients, possible non-thermal hyperfine structure populations, pressure and optical depth effects are shown to be lower than or about 1 m s^{-1} and thus can be neglected

S. A. Levshakov

Physical-Technical Institute, Polytekhnicheskaya Str. 26, 194021 St. Petersburg, Russia, e-mail: lev@astro.ioffe.rssu.ru

P. Molaro

INAF-Osservatorio Astronomico di Trieste, Via G. B. Tiepolo 11, 34143 Trieste, Italy, e-mail: molaro@oats.inaf.it

M. G. Kozlov

Petersburg Nuclear Physics Institute, 188300 Gatchina, Russia, e-mail: mgk@mf1309.spb.edu

A. V. Lapinov

Institute for Applied Physics, Uljanov Str. 46, 603950 Nizhny Novgorod, Russia, e-mail: lapinov@appl.sci-nnov.ru

C. Henkel

Max-Planck-Institut für Radioastronomie, Auf dem Hügel 69, D-53121 Bonn, Germany, e-mail: p220hen@mpifr-bonn.mpg.de

D. Reimers

Hamburger Sternwarte, Universität Hamburg, Gojenbergsweg 112, D-21029 Hamburg, Germany, e-mail: st2e101@hs.uni-hamburg.de

T. Sakai

Institute of Astronomy, The University of Tokyo, Osawa, Mitaka, Tokyo 181-0015, Japan, e-mail: sakai@ioa.s.u-tokyo.ac.jp

I. I. Agafonova

Physical-Technical Institute, Polytekhnicheskaya Str. 26, 194021 St. Petersburg, Russia, e-mail: ira@astro.ioffe.rssu.ru

in the total error budget. The reproducibility of ΔV at the same facility (Effelsberg telescope) on a year-to-year basis is found to be very good. Since the frequencies of the inversion and rotational transitions have different sensitivities to variations in $\mu \equiv m_e/m_p$, the revealed non-zero ΔV may imply that μ changes when measured at high (terrestrial) and low (interstellar) matter densities as predicted by chameleon-like scalar field models – candidates to the dark energy carrier. Thus we are testing whether scalar field models have chameleon-type interactions with ordinary matter. The measured velocity offset corresponds to the ratio $\Delta\mu/\mu \equiv (\mu_{\text{space}} - \mu_{\text{lab}})/\mu_{\text{lab}}$ of $(26 \pm 3) \times 10^{-9} (1\sigma)$.

1 Introduction

This contribution sums up our results of differential measurements of the electron-to-proton mass ratio, $\mu = m_e/m_p$, carried out at the 32-m Medicina, 45-m Nobeyama, and 100-m Effelsberg telescopes [24, 29, 25, 26]. With high spectral resolution (FWHM $\sim 30\text{-}40 \text{ m s}^{-1}$), we observed narrow emission lines (FWHM $< 200 \text{ m s}^{-1}$) of N-bearing molecules arising in cold and dense molecular cores of starless molecular clouds located in the Milky Way. The cores are characterized by low kinetic temperatures $T_{\text{kin}} \sim 10 \text{ K}$, gas densities $n \sim 10^4 - 10^5 \text{ cm}^{-3}$, magnetic fields $B < 10 \mu\text{G}$, and ionization degrees $x_e \sim 10^{-9}$ [8]. The objective of this study is to probe the value of $\Delta\mu/\mu \equiv (\mu_{\text{space}} - \mu_{\text{lab}})/\mu_{\text{lab}}$ which is predicted to be variable when measured at high (laboratory) and low (space) matter density environments [33].

A hypothetical variability of μ is thought to be due to the scalar fields – candidates to the dark energy carrier, – which are ultra-light in cosmic vacuum but possess an effectively large mass locally when they are coupled to ordinary matter by the so-called chameleon mechanism [16]. Several possibilities to detect chameleons were discussed in [2, 7]. First laboratory experiments constraining these models have been recently carried out at Fermilab [42] and in the Lawrence Livermore National Laboratory [38].

A subclass of chameleon models considers the couplings of a scalar field to matter much stronger than gravitational and predicts that fundamental physical quantities such as elementary particle masses may depend on the local matter density, ρ , [33]. This means that a nonzero value of $\Delta\mu/\mu$ is to be expected for all interstellar clouds irrespective of their position and local matter density because the difference $\Delta\rho$ between the terrestrial environment in laboratory measurements and dense interstellar molecular clouds is extremely large, $\rho_{\oplus}/\rho_{\text{cloud}} > 10^{10}$.

In the standard model (SM) of particle physics the dimensionless mass ratio $\mu = m_e/m_p$ defines the ratio of the electroweak scale to the strong scale since the mass of the electron m_e is proportional to the Higgs vacuum expectation value and the mass of the proton m_p is proportional to the quantum chromodynamics scale Λ_{QCD} [5]. The SM is extremely successful in explaining laboratory physics, but it has serious problems in astrophysics where it completely fails to explain dark matter and dark energy. There are many extensions of the SM including supersymmetry and different

multidimensional theories which introduce new particles as possible candidates for the dark matter and additional scalar fields to describe the nature of dark energy.

A concept of dark energy with negative pressure appeared in physics long before the discovery of the accelerating universe through observations of nearby and distant Type Ia Supernovae [36, 37]. Early examples of dark energy in the form of a scalar field with a self-interaction potential can be found in reviews [3] and [35]. If masses of the elementary particles are affected by scalar fields, one can probe the dimensionless constant μ at different physical conditions by means of high precision spectral observations. Namely, since the inversion and rotational molecular transitions have different sensitivities to variations in μ [9], a nonzero $\Delta\mu/\mu$ causes an offset between the radial velocities ($\Delta V \equiv V_{\text{rot}} - V_{\text{inv}}$) of *co-spatially* distributed molecules, which, in turn, provide a measure of $\Delta\mu/\mu$. When the inversion line belongs to NH_3 we will herein call this procedure the ammonia method.

2 The ammonia method

NH_3 is a molecule whose inversion frequencies are very sensitive to changes of μ because of the quantum mechanical tunneling of the N atom through the plane of the H atoms. The inversion vibrational mode of NH_3 is described by a double-well potential, the first two vibrational levels lying below the barrier. The quantum mechanical tunneling splits these two levels into inversion doublets providing a transition frequency that falls into the microwave range [14].

The sensitivity coefficient to μ -variation of the NH_3 $(J, K) = (1, 1)$ inversion transition at 24 GHz is $Q_{\text{inv}} = 4.46$ [9]. This means that the inversion frequency scales as

$$(\Delta\omega/\omega)_{\text{inv}} \equiv (\tilde{\omega} - \omega)/\omega = 4.46(\Delta\mu/\mu), \quad (1)$$

where ω and $\tilde{\omega}$ are the frequencies corresponding to the laboratory value of μ and to an altered μ in a low-density environment, respectively. In other words, the inversion transition sensitivity to μ -variation is 4.46 times higher than that of molecular rotational transitions, where $Q_{\text{rot}} = 1$ and thus,

$$(\Delta\omega/\omega)_{\text{rot}} = \Delta\mu/\mu. \quad (2)$$

In astronomical spectra, any frequency shift $\Delta\omega$ is related to the radial velocity shift ΔV_r (V_r is the line-of-sight projection of the velocity vector)

$$\Delta V_r/c \equiv (V_r - V_0)/c = (\omega_{\text{lab}} - \omega_{\text{obs}})/\omega_{\text{lab}}, \quad (3)$$

where V_0 is the reference radial velocity, c is the speed of light and ω_{lab} , ω_{obs} are the laboratory and observed frequencies, respectively. Therefore, by comparing the apparent radial velocity V_{inv} for the NH_3 inversion transition with the apparent radial velocity V_{rot} for rotational lines originating in the same molecular cloud and moving with radial velocity V_0 with respect to the local standard of rest, one can find from

Eqs. (1 - 3)

$$\Delta\mu/\mu = 0.289(V_{\text{rot}} - V_{\text{inv}})/c \equiv 0.289\Delta V/c . \quad (4)$$

The velocity offset ΔV in Eq.(4) can be expressed as the sum of two components

$$\Delta V = \Delta V_{\mu} + \Delta V_n , \quad (5)$$

where ΔV_{μ} is the shift due to μ -variation and ΔV_n is a random component caused by the inhomogeneous distribution of molecules, turbulent motions and velocity gradients, possible non-thermal hyperfine structure populations, pressure and optical depth effects, and instrumental imperfections (the so-called *Doppler noise*).

We will assume that the Doppler noise component has a zero mean, $\langle \Delta V_n \rangle = 0$ km s⁻¹, and a finite variance, $\text{Var}(\Delta V_n) < \infty$. Then, the signal ΔV_{μ} can be estimated statistically by averaging over a data sample

$$\langle \Delta V \rangle = \langle \Delta V_{\mu} \rangle , \quad (6)$$

and

$$\text{Var}(\Delta V) = \text{Var}(\Delta V_{\mu}) + \text{Var}(\Delta V_n) . \quad (7)$$

Equation (7) shows that the measurability of the signal $\langle \Delta V_{\mu} \rangle$ depends critically on the value of the Doppler noise, $\text{Var}(\Delta V_n)$. The Doppler noise can be reduced by the appropriate choice of molecular lines and molecular clouds.

To have similar Doppler velocity shifts the chosen molecular transitions should share as far as possible the same volume elements. NH₃ inversion transitions are usually detected in dense molecular cores ($n \sim 10^4 - 10^5$ cm⁻³). Mapping of these cores in different molecular lines shows that there is a good correlation between the NH₃, N₂H⁺, and HC₃N distributions [10, 15, 41, 34]. However, in some clouds NH₃ is not traced by HC₃N. The most striking case is the dark cloud TMC-1, where peaks of line emissions are offset by 7 arcmin [32]. Such a chemical differentiation together with velocity gradients within molecular cores is the main source of the unavoidable Doppler noise in Eq.(5). Additional scatter in the ΔV_n values may be caused by the different optical depths of the hyperfine structure transitions and by external electric and magnetic fields discussed below.

3 Selection of targets

To minimize the Doppler noise component in Eq.(5), a preliminary selection of molecular cores suitable for the most precise measurements of the velocity offsets ΔV between rotational and inversion transitions is required. In general, molecular cores are not ideal spheres and when observed at high angular resolutions they frequently exhibit complex substructures. The line profiles may be asymmetric because of non-thermal bulk motions. Taking this into account, we formulate the following selection criteria:

1. The line profiles are symmetric and well described by a single-component Gaussian model. This selection increases the accuracy of the line center measurement. Multiple line components may shift the barycenter and affect the velocity difference between molecular transitions because, e.g., the ratio $\text{NH}_3/\text{HC}_3\text{N}$ may vary from one component to another.
2. The line widths do not exceed greatly the Doppler width caused by the thermal motion of material, i.e., the non-thermal components (infall, outflow, tidal flow, turbulence) do not dominate the line broadening. This ensures that selected molecular lines correspond to the same kinetic temperature and arise co-spatially. For the molecules in question we require the ratio of the Doppler b -parameters to be $\beta = b(\text{NH}_3)/b(\text{HC}_3\text{N})$ or $\beta = b(\text{NH}_3)/b(\text{N}_2\text{H}^+)$, be $\beta \geq 1$.
3. The spectral lines are sufficiently narrow ($b \sim 0.1 - 0.2 \text{ km s}^{-1}$) for the hyperfine structure (hfs) components to be resolved. This allows us to validate the measured radial velocity by means of different hfs lines of the same molecular transition.
4. The spectral lines are not heavily saturated and their profiles are not affected by optical depth effects. The total optical depth of the NH_3 hf transitions is $\tau \leq 10$, i.e., the optical depth of the strongest hf component is $\lesssim 1$.

The kinetic temperature T_{kin} , and the nonthermal (turbulent) velocity dispersion, σ_{turb} , can be estimated from the line broadening Doppler parameters $b = \sqrt{2}\sigma_v$, of, e.g., the NH_3 (1,1) and HC_3N (2-1) lines. Here σ_v is the line of sight velocity dispersion of the molecular gas within a given cloud. If the two molecular transitions trace the same material and have the same nonthermal velocity component, σ_v is the quadrature sum of the thermal σ_{th} and turbulent σ_{turb} velocity dispersions. In this case a lighter molecule with a mass m_l should have a line width wider than with a heavier molecule with $m_h > m_l$.

For thermally dominated line widths ($\beta > 1$) and co-spatially distributed species we obtain the following relations (e.g., [10]):

$$T_{\text{kin}} = m_l m_h (\sigma_l^2 - \sigma_h^2) / k(m_h - m_l), \quad (8)$$

and

$$\sigma_{\text{turb}}^2 = (m_h \sigma_h^2 - m_l \sigma_l^2) / (m_h - m_l), \quad (9)$$

where k is Boltzmann's constant, and the thermal velocity dispersion σ_{th} is given by

$$\sigma_{\text{th},i} = (kT_{\text{kin}}/m_i)^{1/2}. \quad (10)$$

It should be noted that HC_3N is usually distributed in a volume of the molecular core larger than NH_3 since N-bearing molecules trace the inner core, whereas C-bearing molecules occupy the outer part [8]. Such a differentiation may cause a larger non-thermal component in the velocity distribution of HC_3N . If both molecules are shielded from external incident radiation, and the gas temperature mainly comes from heating by cosmic rays, then a formal application of Eqs.(8) and (9) to the apparent line widths provides a lower limit on T_{kin} and an upper limit on σ_{turb} . In molecular cores where the only source of heating are the cosmic rays and the cooling comes from the line radiation mainly from CO , a lower bound on the kinetic temper-

ature is about 8 K [11]. Thus, point 2 of the selection criteria requires $T_{\text{kin}} \sim 8\text{-}10$ K if both lighter and heavier molecules are distributed co-spatially.

4 Preliminary results

In our preliminary single-pointing observations [25] we studied 41 molecular cores along 55 lines of sight. The $\text{NH}_3(1,1)$, $\text{HC}_3\text{N}(2-1)$, and $\text{N}_2\text{H}^+(1-0)$ transitions were observed with the 100-m Effelsberg, 32-m Medicina, and 45-m Nobeyama telescopes. The analysis of the total sample revealed large systematic shifts and ‘heavy tails’ of the ΔV probability distribution function resulting in a poor concordance between three mean values: the weighted mean $\langle \Delta V \rangle_{\text{w}} = 27.4 \pm 4.4 \text{ m s}^{-1}$ (weights inversionally proportional to the variances), the robust redescending M -estimate $\langle \Delta V \rangle_{\text{M}} = 14.1 \pm 4.0 \text{ m s}^{-1}$, and the median $\Delta V_{\text{med}} = 17 \text{ m s}^{-1}$. The scatter in the ΔV values reflects effects related to the gas kinematics and the chemical segregation of one molecule with respect to the other (approximately 50% of the targets showed $\beta < 1$).

If we now consider molecular lines that fulfill the selection criteria, the sample size is $n = 23$, i.e. two times smaller than the total data set. Nevertheless, for this reduced sample we obtained better concordance: $\langle \Delta V \rangle_{\text{w}} = 20.7 \pm 3.0 \text{ m s}^{-1}$, $\langle \Delta V \rangle_{\text{M}} = 21.5 \pm 2.8 \text{ m s}^{-1}$, and $\Delta V_{\text{med}} = 22 \text{ m s}^{-1}$.

In this preliminary study we found 7 sources with thermally dominated motions which provide $\langle \Delta V \rangle_{\text{w}} = 21.1 \pm 1.3 \text{ m s}^{-1}$, $\langle \Delta V \rangle_{\text{M}} = 21.2 \pm 1.8 \text{ m s}^{-1}$, and $\Delta V_{\text{med}} = 22 \text{ m s}^{-1}$.

The most accurate result was obtained with the Effelsberg 100-m telescope: $\Delta V = 27 \pm 4_{\text{stat}} \pm 3_{\text{sys}} \text{ m s}^{-1}$ (the value is slightly corrected in [26]). The systematic error in this estimate is due to uncertainties of the rest frequencies of the $\text{HC}_3\text{N}(2-1)$ hfs transitions since uncertainties of the $\text{NH}_3(1,1)$ hfs transitions are less than 1 m s^{-1} [21]. When interpreted in terms of the electron-to-proton mass ratio variation, this gives $\Delta\mu/\mu = (26 \pm 4_{\text{stat}} \pm 3_{\text{sys}}) \times 10^{-9}$.

Thus, for the first time we obtained an astronomical spectroscopic estimate of the relative change in the fundamental physical constant μ at the level of 10^{-9} which is 10^3 times more sensitive than the upper limits on $\Delta\mu/\mu$ obtained by the ammonia method from extragalactic observations [9, 30, 28, 13].

5 Mapping of cold molecular cores in NH_3 and HC_3N lines

In this section we report on new observations in which we measure ΔV at different positions across individual clouds in order to test the reproducibility of the velocity offsets in the presence of large-scale velocity gradients [26]. From the list of molecular cores observed with the Effelsberg 100-m telescope, we selected several objects with symmetric profiles of the $\text{NH}_3(1,1)$ and $\text{HC}_3\text{N}(2-1)$ hfs transi-

tions. In these objects the line widths are thermally dominated, i.e., the parameter $\beta = \sigma_v(\text{NH}_3)/\sigma_v(\text{HC}_3\text{N}) \geq 1$. The chosen targets are the molecular cores L1498, L1512, L1517B, and L1400K, which have already been extensively studied in many molecular lines [1, 22, 23, 41, 40, 6].

The inversion line of ammonia $\text{NH}_3(1,1)$ at 23.694 GHz and the rotation line of cyanoacetylene $\text{HC}_3\text{N}(2-1)$ at 18.196 GHz were measured with a K-band HEMT (high electron mobility transistor) dual channel receiver, yielding spectra with an angular resolution of HPBW $\sim 40''$ in two orthogonally oriented linear polarizations. The measurements were carried out in frequency-switching mode using a frequency throw of 5 MHz. The backend was an FFTS (Fast Fourier Transform Spectrometer) operated with its minimum bandwidth of 20 MHz providing simultaneously 16 384 channels for each polarization. The resulting channel separations are 15.4 m s^{-1} for NH_3 and 20.1 m s^{-1} for HC_3N . We note, however, that the true velocity resolution is about two times lower, FWHM $\sim 30 \text{ m s}^{-1}$ and 40 m s^{-1} , respectively [17]. The sky frequencies were reset at the onset of each scan and the Doppler tracking was used continuously to track Doppler shifts during the observations. Observations started by measuring the continuum emission of calibration sources and continued by performing pointing measurements toward a source close to the spectroscopic target. The calibration is estimated to be accurate to $\pm 15\%$ and the pointing accuracy to be higher than $10''$.

After corrections for the rounded frequencies, the individual exposures were co-added to increase the signal-to-noise ratio S/N. The spectra were folded to remove the effects of the frequency switch, and base lines were determined for each spectrum. The resolved hfs components show no kinematic substructure and consist of an apparently symmetric peak profile without broadened line wings or self-absorption features. The line parameters, such as the total optical depth in the transition τ (i.e., the peak optical depth if all hyperfine components were placed at the same velocity), the radial velocity V_{lsr} , the line broadening Doppler parameter b , and the amplitude A , were obtained through fitting of the *one-component* Gaussian model to the observed spectra:

$$T(v) = A \cdot [1 - \exp(-t(v))], \quad (11)$$

with

$$t(v) = \tau \cdot \sum_{i=1}^k a_i \exp [-(v - v_i - V_{lsr})^2 / b^2], \quad (12)$$

which transforms for optically thin transitions into

$$T(v) = A' \cdot \sum_{i=1}^k a_i \exp [-(v - v_i - V_{lsr})^2 / b^2]. \quad (13)$$

The sum in (12) and (13) runs over the $k = 18$ and $k = 6$ hfs components of the $\text{NH}_3(1,1)$ and $\text{HC}_3\text{N}(2-1)$ transitions, respectively.

To test possible optical depth effects, we calculated two sets of the fitting parameters: (1) based on the analysis of only optically thin satellite lines with $\Delta F_1 \neq 0$,

and (2) obtained from the fit to the entirety of the $\text{NH}_3(1,1)$ spectrum including the main transitions with $\Delta F_1 = 0$, which have optical depths $\tau \approx 1-2$, as can be inferred from the relative intensities of the hfs components. The resulting V_{lsr} values for all targets were within the 1σ uncertainty intervals.

To control another source of errors caused by instrumental imperfections, we carried out *repeated* observations at 10 offset positions: two in L1498, L1517B, and L1400K, respectively, and four in L1512. The ΔV dispersion resulting from these repeated measurements is $\sigma(\Delta V) = 2.0 \text{ m s}^{-1}$. This dispersion is lower than the calculated 1σ errors of the individual ΔV values, which ensures that we are not missing any significant instrumental errors at the level of a few m s^{-1} .

We also checked the velocity offsets ΔV obtained in our observations with the 100-m Effelsberg telescope in Feb 2009 and Jan 2010. The reproducibility of the velocity offsets at the same facility on a year-to-year base is very good for L1498, L1512 and L1517B (concordance within 1σ uncertainty intervals), except for L1400K where the central point is probably an outlier.

The comparison of the velocity dispersions determined from the $\text{NH}_3(1,1)$ and $\text{HC}_3\text{N}(2-1)$ lines did not show any significant variations with position within each molecular core. All data are consistent with thermally dominated line broadening. In particular, the following weighted mean values were determined: $\beta_{\text{L1498}} = 1.24 \pm 0.03$, $\beta_{\text{L1512}} = 1.32 \pm 0.05$, $\beta_{\text{L1517B}} = 1.11 \pm 0.01$, and $\beta_{\text{L1400K}} = 1.23 \pm 0.04$. The weighted mean values of the velocity dispersions for NH_3 range between $\sigma_{\text{L1512}} = 78 \pm 1 \text{ m s}^{-1}$ and $\sigma_{\text{L1400K}} = 86 \pm 1 \text{ m s}^{-1}$, and for HC_3N between $\sigma_{\text{L1512}} = 59 \pm 2 \text{ m s}^{-1}$ and $\sigma_{\text{L1517B}} = 74 \pm 1 \text{ m s}^{-1}$. This can be compared with the speed of sound inside a thermally dominated region of a cold molecular core that is defined as (e.g., [39])

$$v_s = (kT_{\text{kin}}/m_0)^{1/2}, \quad (14)$$

where m_0 is the mean molecular mass. With $m_0 \approx 2.3 \text{ amu}$ for molecular clouds, one has $v_s \approx 60\sqrt{T_{\text{kin}}} \text{ m s}^{-1}$, which shows that at the typical kinetic temperature of 10 K the nonthermal velocities are in general subsonic, and that the selected targets do represent the quiescent material at different distances from the core centers.

The gas temperature in the molecular cores was estimated from the apparent line widths using Eq. (8). For L1498 we obtained a lower limit on the kinetic temperature $T_{\text{kin}} = 7.1 \pm 0.5 \text{ K}$ (average over 8 points), which is slightly lower than $T_{\text{kin}} = 10 \text{ K}$ measured by a different method from the relative populations of the $(J, K) = (2, 2)$ and $(1, 1)$ levels of NH_3 described by the rotational temperature T_{R}^{21} [41]. For L1512 the temperature averaged over 11 points is $T_{\text{kin}} = 9.6 \pm 0.6 \text{ K}$, which is consistent with the value of 10 K. The kinetic temperatures in the L1517B core in all measured positions is well below 9.5 K – the value from [41], which means that the nonthermal velocity dispersions of NH_3 and HC_3N differ significantly and that both species *do not trace* the same material. The three scanned points in the L1400K core showed $T_{\text{kin}} = 8.3 \pm 3.2 \text{ K}$ – close to the expected value of 10 K (measurements of the gas temperature in this core were not performed in previous studies).

We found that, in general, the spatial fluctuations of T_{kin} do not exceed a few kelvin implying uniform heating and absence of the localized heat sources. The

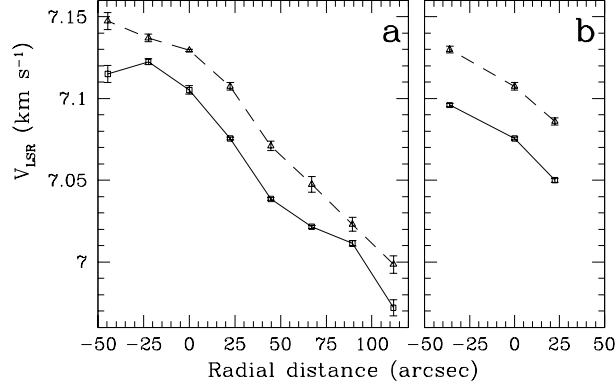


Fig. 1 Example of the line-of-sight velocities of NH_3 ($J, K = (1, 1)$) (squares) and $\text{HC}_3\text{N } J = 2 - 1$ (triangles) at different radial distances along the main diagonal cut (panel **a**) and in the perpendicular direction (panel **b**) of the molecular core L1512. Shown are 1σ error bars. For more detail, see [26].

kinetic temperature tends to rise with the distance from the core center, which is in line with the results from [41].

The radial velocity profiles along the different diagonal cuts toward the selected targets are shown in Figs. 3 and 4 in [26]. The diagonal cut in L1498 exhibits coherently changing velocities of $V_{lsr}(\text{HC}_3\text{N})$ and $V_{lsr}(\text{NH}_3)$ except one point at the core edge. The velocity gradient is small, $|\nabla V_{lsr}| \approx 0.5 \text{ km s}^{-1} \text{ pc}^{-1}$. This picture coincides with the previously obtained results based on observations of CO, CS, N_2H^+ and NH_3 in this core and was interpreted as an inward flow [22, 41]. Taken together, all available observations classify L1498 as one of the most quiet molecular cores. Thus, we can expect that the Doppler noise (irregular random shifts in the radial velocities between different transitions) is minimal in this core.

In L1512, the $V_{lsr}(\text{NH}_3)$ and $V_{lsr}(\text{HC}_3\text{N})$ distributions are almost parallel (Fig. 1). The same kinematic picture was obtained for this core in [22] from observations of CS and NH_3 lines and interpreted as a simple rotation around the center. The velocity gradients derived from both NH_3 and HC_3N lines are similar, $\nabla V_{lsr} \approx 1.5 \text{ km s}^{-1} \text{ pc}^{-1}$, and consistent with the gradient based on N_2H^+ measurements in [4]. This means that NH_3 , HC_3N , and N_2H^+ trace the same gas, so the Doppler shifts ΔV between them should be insignificant.

In the core L1517B, which is known to be very compact [22], we only observed the central $30'' \times 30''$ where the velocities of NH_3 and HC_3N along two perpendicular cuts do not change much: $\nabla V_{lsr}(\text{NH}_3) \approx 0.3 \text{ km s}^{-1} \text{ pc}^{-1}$, $\nabla V_{lsr}(\text{HC}_3\text{N}) \approx 0.8 \text{ km s}^{-1} \text{ pc}^{-1}$, and in the perpendicular direction $\nabla V_{lsr}(\text{NH}_3) \approx \nabla V_{lsr}(\text{HC}_3\text{N}) \approx -0.8 \text{ km s}^{-1} \text{ pc}^{-1}$. However, a wider area observation ($\approx 80'' \times 80''$) of this core revealed an outward gas motion at the core periphery with a higher velocity gradient, $\nabla V_{lsr}(\text{N}_2\text{H}^+) \approx 1.1 \text{ km s}^{-1} \text{ pc}^{-1}$ [41], which is consistent with earlier results on NH_3 observations [12]. This can lead to an additional shift in the radial velocity of

HC₃N line since, in general, the C-bearing molecules also trace a lower density gas component ($n < 10^4 \text{ cm}^{-3}$) in the envelope of the molecular core. A higher nonthermal velocity dispersion of the HC₃N line than for NH₃ has already been mentioned above in regard to the temperature measurements in this core.

In L1400K we only observed three positions. Both molecules trace the same gradient of $\nabla V_{lsr} \approx 1.9 \text{ km s}^{-1} \text{ pc}^{-1}$, which is in line with $\nabla V_{lsr}(\text{N}_2\text{H}^+) = 1.8 \pm 0.1 \text{ km s}^{-1} \text{ pc}^{-1}$ derived in [4]. The mapping in different molecular lines in [41] revealed that L1400K deviates significantly from spherical symmetry and exhibits quite a complex kinematic structure. In particular, the distributions of N₂H⁺ and NH₃ do not coincide: N₂H⁺ has an additional component to the west of the center. This explains why [6] reported a blue-ward skewness for this core, $\theta = -0.42 \pm 0.10$, in the the N₂H⁺ (1–0) hfs profiles, whereas in our observations the NH₃(1,1) hfs transitions are fully symmetric: at the central position the skewness of the resolved and single hfs component $F_1, F = 0, \frac{1}{2} \rightarrow 1, 1\frac{1}{2}$ of NH₃ is $\theta = -0.1 \pm 0.3$.

Our current measurements show very similar velocity shifts $\langle \Delta V \rangle_M = 25.8 \pm 1.7 \text{ m s}^{-1}$ and $28.0 \pm 1.8 \text{ m s}^{-1}$ (M -estimates) for, respectively, the cores L1498 and L1512 where the Doppler noise reaches minimal levels. A higher shift $\langle \Delta V \rangle_M = 46.9 \pm 3.3 \text{ m s}^{-1}$ is observed in the L1517B core – again in accord with its revealed kinematic structure, which allows us to expect a higher radial velocity for the HC₃N line. On the other hand, a lower value $\langle \Delta V \rangle_M = 8.5 \pm 3.4 \text{ m s}^{-1}$ in L1400K may come from the irregular kinematic structure of the core center, which could increase the radial velocity of the NH₃ line.

Thus, as reference velocity offset we chose the most robust M -estimate of the mean value from the L1498 and L1512 cores: $\langle \Delta V \rangle_M = 26.9 \pm 1.2_{\text{stat}} \text{ m s}^{-1}$. Taking into account that the uncertainty of the HC₃N(2–1) rest frequency is about 3 m s^{-1} , whereas that of NH₃(1,1) is less than 1 m s^{-1} , we finally have $\langle \Delta V \rangle_M = 26.9 \pm 1.2_{\text{stat}} \pm 3.0_{\text{sys}} \text{ m s}^{-1}$. When it is interpreted in terms of the electron-to-proton mass ratio variation, as defined in Eq.(4), this velocity offset provides $\Delta\mu/\mu = (26 \pm 1_{\text{stat}} \pm 3_{\text{sys}}) \times 10^{-9}$.

6 Discussion and conclusions

In two molecular cores with the lowest Doppler noise L1498 and L1512, we register very close values of the velocity offset $\Delta V \sim 27 \text{ m s}^{-1}$ between the rotational transition HC₃N(2–1) and the inversion transition NH₃(1,1). These values coincide with the most accurate estimate obtained from the Effelsberg dataset on 12 molecular clouds in the Milky Way [25]. Two other cores, L1517B and L1400K, exhibit velocity shifts that are either higher ($\sim 47 \text{ m s}^{-1}$ in L1517B) or lower ($\sim 9 \text{ m s}^{-1}$ in L1400K) than the mean value, but the positive (L1517B) and negative (L1400K) deflections from the mean can be explained from the observed kinematics in these cores.

Of course, simultaneous observations of the NH₃(1,1) inverse transition and rotational transitions of some N-bearing molecules, such as N₂H⁺(1–0) and N₂D⁺(1–0)

would give a more accurate test. The main obstacle to this way is that the laboratory frequencies of N_2H^+ and N_2D^+ are known with accuracies not better than 14 m s^{-1} [25]. Using the N_2H^+ rest frequency from the Cologne Database for Molecular Spectroscopy (CDMS) [31] and observing with the Nobeyama 45-m telescope, we obtained a velocity shift between N_2H^+ and NH_3 of $23.0 \pm 3.4 \text{ m s}^{-1}$ in L1498, $24.5 \pm 4.3 \text{ m s}^{-1}$ in L1512, and $21.0 \pm 5.1 \text{ m s}^{-1}$ in L1517B [25]. We note that similar shifts are indicated for the central parts of L1498 and L1517B in Fig. 11 in [41], where these targets were observed with the 30-m IRAM telescope also using an N_2H^+ rest frequency which is very close to the CDMS value.

Obviously, for more definite conclusions, new laboratory measurements of the rest frequencies and new observations involving other targets and other molecular transitions with different sensitivity coefficients Q are required. It has already been suggested to measure Λ -doublet lines of the light diatomic molecules OH and CH [18], microwave inversion-rotational transitions in the partly deuterated ammonia NH_2D and ND_2H [19], low-lying rotational transitions in ^{13}CO and the fine-structure transitions in C I [27], and tunneling and rotation transitions in the hydronium ion H_3O^+ [20]. The fourth opportunity is of particular interest since the rest-frame frequencies of H_3O^+ transitions are very sensitive to the variation of μ , and their sensitivity coefficients have *different* signs. For example, the two lowest frequency transitions $J_K = 1_1^- \rightarrow 2_1^+$ and $J_K = 3_2^+ \rightarrow 2_2^-$ of para- H_3O^+ at, respectively, 307 and 364 GHz have $\Delta Q = Q_{307} - Q_{364} = 14.7$, which is 4 times larger than $\Delta Q = 3.46$ from the ammonia method. This means that the offset $\Delta V \sim 27 \text{ m s}^{-1}$, detected with the ammonia method, should correspond to a relative velocity shift between these transitions, $\Delta V = V_{364} - V_{307}$, of about 100 m s^{-1} if $\Delta\mu/\mu \approx 26 \times 10^{-9}$. We consider the hydronium method [20] as an important independent test of the $\Delta\mu/\mu$ value in the Milky Way.

To conclude, we note that in cold molecular cores with low ionization degrees ($x_e \sim 10^{-8} - 10^{-9}$) frequency shifts caused by external electric and magnetic fields and by the cosmic black body radiation-induced Stark effect are less or about 1 m s^{-1} and cannot affect the revealed nonzero velocity offset between the rotational and inversion transitions in the ammonia method. Detailed calculations of these effects are given in [26].

Our current results tentatively support the hypothesis that the fundamental physical constant – the electron-to-proton mass ratio – may differ in low-density environments from its terrestrial value. This may be the consequence of the chameleon-like scalar field. However, new laboratory measurements of the molecular rest frequencies and new observations involving other molecular transitions and other targets are required to reach more definite conclusions.

Acknowledgements We are grateful to the staffs of the Medicina 32-m, Nobeyama 45-m, and Effelsberg 100-m radio telescope observatories for excellent support in our observations. We thank Gabriella Schiulaz for her kind assistance in preparing the text. The project has been supported in part by DFG Sonderforschungsbereich SFB 676 Teilprojekt C4, the RFBR grants No. 09-02-12223, 09-02-00352, and 08-02-92001, the Federal Agency for Science and Innovations grant NSh-3769.2010.2, the Program IV.12/2.5 of the Physical Department of the RAS.

References

1. P. J. Benson, P. C. Myers, *ApJS*, **71**, 89 (1989)
2. C. Burrage, A.-C. Davis, D. J. Shaw, *Phys. Rev. D*, **79**, 044028 (2009)
3. R. R. Caldwell, R. Dave, P. J. Steinhardt, *Phys. Rev. Lett.*, **80**, 1582 (1998)
4. P. Caselli, P. J. Benson, P. C. Myers, M. Tafalla, *ApJ*, **572**, 238 (2002)
5. C., Chin, V. V. Flambaum, M. G. Kozlov, *New J. Phys.*, **11**, 055048 (2009)
6. A. Crapsi, P. Caselli, C. M. Walmsley, et al., *ApJ*, **619**, 379 (2005)
7. A. Davis, C. A. O. Schelpe, D. J. Shaw, *Phys. Rev. D*, **80**, 064016 (2009)
8. J. Di Francesco, N. J. Evans, II, P. Caselli, et al., in *Protostars and Planets. V*, eds. B. Reipurth, D. Jewitt, and K. Keil (Uni. Arizona Press, Tucson, 2007), p. 17
9. V. V. Flambaum, M. G. Kozlov, *Phys. Rev. Lett.*, **98**, 240801 (2007)
10. G. A. Fuller, P. C. Myers, *ApJ*, **418**, 273 (1993)
11. P. F. Goldsmith, W. D. Langer, *ApJ*, **222**, 881 (1978)
12. A. A. Goodman, P. J. Benson, G. A. Fuller, P. C. Myers, *ApJ*, **406**, 528 (1993)
13. C. Henkel, K. M. Menten, M. T. Murphy, M. T., et al., *A&A*, **500**, 725 (2009)
14. P. T. P. Ho, C. H. Townes, *ARA&A*, **21**, 239 (1983)
15. S. Hotzel, J. Harju, C. M. Walmsley, *A&A*, **415**, 1065 (2004)
16. J. Khoury, A. Weltman, *Phys. Rev. Lett.*, **93**, 171104 (2004)
17. B. Klein, S. D. Philipp, R. Güsten, et al., *Proc. of the SPIE*, **6275**, 627511 (2006)
18. M. G. Kozlov, *Phys. Rev. A*, **80**, 022118 (2009)
19. M. G. Kozlov, A. V. Lapinov, S. A. Levshakov, *J. Phys. B*, **43**, 074003 (2010)
20. M. G. Kozlov, S. A. Levshakov, *ApJ*, in press (2010)
21. S. G. Kukolich, *Phys. Rev.*, **156**, 83 (1967)
22. C. W. Lee, P. C. Myers, M. Tafalla, *ApJS*, **136**, 703 (2001)
23. J.-E. Lee, N. J. Evans, II, Y. L. Shirley, K. Tatematsu, *ApJ*, **583**, 789 (2003)
24. S. A. Levshakov, P. Molaro, M. G. Kozlov, eprint arXiv:0808.0583 (2008)
25. S. A. Levshakov, P. Molaro, A. V. Lapinov, et al., *A&A*, **512**, 44 (2010)
26. S. A. Levshakov, A. V. Lapinov, C. Henkel, et al., *A&A*, in press (2010)
27. S. A. Levshakov, P. Molaro, P., D. Reimers, *D. A&A*, **516**, 113 (2010)
28. K. M. Menten, R. Güsten, S. Leurini, et al., *A&A*, **492**, 725 (2008)
29. P. Molaro, S. A. Levshakov, M. G. Kozlov, *Nuc. Phys. B Proceed. Suppl.*, **194**, 287 (2009)
30. M. T. Murphy, V. V. Flambaum, S. Muller, C. Henkel, *Sci.*, **320**, 1611 (2008)
31. H. S. P. Müller, F. Schlöder, J. Stutzki, G. Winnewisser, *J. Mol. Struct.*, **742**, 215 (2005)
32. C. A. Olano, C. M. Walmsley, T. L. Wilson, *A&A*, **196**, 194 (1988)
33. K. A. Olive, M. Pospelov, *Phys. Rev. D*, **77**, 043524 (2008)
34. L. Pagani, F. Daniel, M.-L. Dubernet, *A&A*, **494**, 719 (2009)
35. P. J. E. Peebles, B. Ratra, *Rev. Mod. Phys.*, **75**, 559 (2003)
36. S. Perlmutter, G. Aldering, M. della Valle, et al., *Nature*, **391**, 51 (1998)
37. A. G. Riess, A. V. Filippenko, P. Challis, P., et al., *AJ*, **116**, 1009 (1998)
38. G. Rybka, M. Hotz, L. J. Rosenberg, et al., *Phys. Rev. Lett.*, **105**, 051801 (2010)
39. F. H. Shu, *ApJ*, **214**, 488 (1977)
40. M. Tafalla, J. Santiago, P. C. Myers, et al., *A&A*, **455**, 577 (2006)
41. M. Tafalla, P. C. Myers, P. Caselli, C. M. Walmsley, *A&A*, **16**, 191 (2004)
42. A. Upadhye, J. H. Steffen, A. Weltman, *Phys. Rev. D*, **81**, 015013 (2010)